Published in final edited form as:
Biochim Biophys Acta Mol Cell Res. 2017 October 01; 1864(10): 1656–1667. doi:10.1016/j.bbamcr.2017.05.021.

Saccharomyces cerevisiae cells lacking Pex3 contain membrane vesicles that harbor a subset of peroxisomal membrane proteins

Justyna P. Wroblewska[#a], **Luis Daniel Cruz-Zaragoza**[#b], **Yuan Wei**[a], **Andreas Schummer**[c], **Silvia G. Chuartzman**[d], **Rinse de Boer**[a], **Silke Oeljeklaus**[c], **Maya Schuldiner**[d], **Einat Zalckvar**[d], **Bettina Warscheid**[c,e], **Ralf Erdmann**[2,b], **Ida J. van der Klei**[2,a]

[a]Molecular Cell Biology, Groningen Biomolecular Sciences and Biotechnology Institute (BBA) University of Groningen, PO Box 11103, 9300 CC Groningen, The Netherlands [b]Systembiochemie, Institut für Biochemie und Pathobiochemie, Medizinische Fakultät, Ruhr-Universität Bochum, 44801 Bochum, Germany [c]Department of Biochemistry and Functional Proteomics, Institute of Biology II, Faculty of Biology, University of Freiburg, 79104 Freiburg, Germany [d]Department of Molecular Genetics, Weizmann Institute of Science, Rehovot, 7610001, Israel [e]BIOSS Centre for Biological Signalling Studies, University of Freiburg, Germany

[#] These authors contributed equally to this work.

Abstract

Pex3 has been proposed to be important for the exit of peroxisomal membrane proteins (PMPs) from the ER, based on the observation that PMPs accumulate at the ER in *Saccharomyces cerevisiae pex3* mutant cells.

Using a combination of microscopy and biochemical approaches, we show that a subset of the PMPs, including the receptor docking protein Pex14, localizes to membrane vesicles in *S. cerevisiae pex3* cells. These vesicles are morphologically distinct from the ER and do not co-sediment with ER markers in cell fractionation experiments. At the vesicles, Pex14 assembles with other peroxins (Pex13, Pex17, and Pex5) to form a complex with a composition similar to the PTS1 import pore in wild-type cells.

Fluorescence microscopy studies revealed that also the PTS2 receptor Pex7, the importomer organizing peroxin Pex8, the ubiquitin conjugating enzyme Pex4 with its recruiting PMP Pex22, as well as Pex15 and Pex25 co-localize with Pex14. Other peroxins (including the RING finger complex and Pex27) did not accumulate at these structures, of which Pex11 localized to mitochondria. In line with these observations, proteomic analysis showed that in addition to the docking proteins and Pex5, also Pex7, Pex4/Pex22 and Pex25 were present in Pex14 complexes isolated from *pex3* cells. However, formation of the entire importomer was not observed, most likely because Pex8 and the RING proteins were absent in the Pex14 protein complexes.

Our data suggest that peroxisomal membrane vesicles can form in the absence of Pex3 and that several PMPs can insert in these vesicles in a Pex3 independent manner.

[2]Corresponding authors: ralf.erdmann@rub.de; i.j.van.der.klei@rug.nl.

Europe PMC Funders Author Manuscripts

Keywords

peroxisome; organelle; Pex3; peroxisomal membrane protein; protein sorting; endoplasmic reticulum; yeast; *Saccharomyces cerevisiae*

1 Introduction

Peroxisomes are highly dynamic, multifunctional organelles that occur in most eukaryotic cells [1, 2]. It is well established that peroxisomes can multiply by fission and several proteins involved in this process have been identified and characterized in detail [3]. Peroxisomes can also form *de novo* from the endoplasmic reticulum (ER) [4, 5]. However, it is still debated whether this process only occurs in mutant cells lacking pre-existing organelles or also takes place at normal conditions in wildtype (WT) cells [6].

Our current knowledge on the molecular mechanisms involved in *de novo* peroxisome formation from the ER is mainly based on the analysis of organelle formation in cells of yeast *pex3* or *pex19* deletion strains upon re-introduction of the corresponding genes [4]. This model is supported by the outcome of *in vitro* studies, which revealed that vesicles containing peroxisomal membrane proteins (PMPs) bud off from the ER [7, 8].

It has generally been accepted that yeast *pex3* cells fully lack peroxisomal membrane remnants [9, 10]. Because peroxisomes reappear in these cells upon reintroduction of Pex3, they cannot be formed from pre-existing ones and hence should originate *de novo* from another membrane template. Many observations pointed to a role of the ER in this process. It has been proposed that during *de novo* peroxisome formation in *Saccharomyces cerevisiae*, all peroxisomal membrane proteins (PMPs) first sort to the ER and subsequently exit this compartment in two types of vesicles in a Pex3/Pex19 dependent manner [10, 11]. These vesicles subsequently fuse in a Pex1/Pex6 dependent manner to form nascent peroxisomes [11]. This model is in line with the observation that PMPs accumulate at the ER in *S. cerevisiae pex3* cells [10]. However, this result may be related to the fact that in this study PMPs were overproduced, because overproduction of PMPs can result in mistargeting to the ER [12]. Indeed, earlier observations by Hettema and colleagues suggested that in *S. cerevisiae pex3* and *pex19* cells PMP that were not overproduced mislocalized to the cytosol. However, in this study only three PMPs (Pex11, Pat1, Pex15) were analyzed [9]. Unexpectedly, recent studies showed that in *S. cerevisiae pex3* cells Pex11 mislocalizes to mitochondria [13, 14]. Moreover, analysis of *Hansenula polymorpha pex3* mutant cells revealed the presence of peroxisomal membrane structures that contain a subset of the PMPs [15].

These results prompted us to re-investigate the localization of PMPs in *S. cerevisiae pex3* cells. Electron microscopy and subcellular fractionation experiments showed that *pex3* cells contain small vesicular structures that harbor Pex14 and are independent from ER and mitochondria. Fluorescence microscopy analysis of the localization of 19 additional peroxins showed that 9 of them (partially) colocalized with Pex14 (Pex5, Pex7, Pex13, Pex17, Pex8, Pex4, Pex22, Pex15 and Pex25). Proteomic studies indicated that *S. cerevisiae pex3* cells contain the Pex14/Pex13/Pex17-docking complex of the peroxisomal protein

import machinery of a composition that is similar to the WT import pore, but that lacks the RING finger complex proteins (Pex2, Pex10, Pex12) and the AAA-peroxins (Pex1, Pex6) of the exportomer.

Summarizing, our data indicate that in *S. cerevisiae pex3* cells PMPs do not accumulate at the ER, but rather in small peroxisomal membrane vesicles.

2 Materials and methods

2.1 Strains and growth conditions

The *S. cerevisiae* strains used in this study are derivatives of BY4742 or CB199 and are listed inTable S1. *S. cerevisiae* cells were grown at 30°C on either YPD (1% yeast extract, 1% peptone and 1% glucose), selective minimal medium containing 0.67% yeast nitrogen base without amino acids (YNB; Difco BD) or minimal medium supplemented with 1% glucose or a mixture of 0.1% glucose, 0.1% oleic acid, 0.05% Tween-80 (MM-O) [16]. For cell fractionation and complex isolation studies, cells were grown for 8 h in selective medium supplemented with 0.3% glucose, and then oleic acid was added to a final concentration of 0.1% in the presence of 0.05% Tween-40 and incubated for 16 h. For selection of auxotrophic transformants, selective minimal medium was supplemented with 2% glucose and the required amino acids mixture. For growth on agar plates, the medium was supplemented with 2% agar. For selection of antibiotic resistant transformants, YPD plates containing 200 μg/ml Zeocin (Invitrogen), 200 μg/ml Hygromycin B (Invitrogen), 100 μg/ml Nourseothricin (Werner Bioagents) or 300 μg/ml Geneticin-418 (AppliChem) were used. For selection of auxotrophic transformants, minimal medium was supplemented with the required amino acids.

2.2 Molecular techniques

Oligonucleotides used in this study are listed in Table S2. Preparative polymerase chain reactions (PCR) were carried out with Phusion polymerase (Thermo Scientific). Initial selection of positive transformants by colony PCR was carried out using Phire polymerase (Thermo Scientific).

2.3 Western blotting

Total cell extracts were prepared from cells treated with 12.5% trichloroacetic acid (TCA) and used for SDS-polyacrylamide gel electrophoresis and western blotting as detailed previously [17]. Equal amounts of protein were loaded per lane. Nitrocellulose membranes were probed with polyclonal rabbit antibodies raised against Pex3 [18], Pex5 [19], Pex11 [20], Pex13 [21], Pex14 [19], Pex17 [22], Fox3 [23], Por1 [24], Kar2 [25], Pgk1 (Invitrogen, Karlsruhe, Germany), Tim23 [26], pyruvate carboxylase-1 (Pyc1) [27], or glucose-6-phosphate dehydrogenase (G6PD; Sigma-Aldrich). mGFP-fusion proteins of Pex10, Pex11, Pex13, Ant1 were probed with mouse monoclonal antiserum against green fluorescence protein (GFP; Santa Cruz Biotechnology, sc-9996). Anti-rabbit IgG IRDye800CW-conjugated secondary antibody was used and the membranes were visualized with Odyssey® infrared imaging system (LI-COR Bioscience, Bad Homburg, Germany). Anti-

mouse secondary antibodies conjugated to horseradish peroxidase were also used for detection.

2.4 Construction of strains

2.4.1 Construction of BY4742 *pex3* —Deletion of the *PEX3* gene in *S. cerevisiae* BY4742 *pex3* strain was confirmed by colony PCR using primers TER202 and TER203. Next, *ATG1* was disrupted by replacing the *ATG1* region with the nourseothricin resistance gene using a PCR fragment containing the selective marker and 50 bp of *ATG1* flanking regions. The PCR fragment was amplified with the primers TER208 and TER209 using plasmid pAG25 [28] as a template, and then transformed into *pex3* cells. Nourseothricin resistant transformants were selected and the correct integration was checked by colony PCR using the primers TER210 and TER211, and confirmed by Southern blotting.

To obtain *pex3* Pex14-mGFP and *pex3 atg1* Pex14-mGFP, a fragment containing *PEX14-mGFP* was amplified using primers TER216 and TER217 from the yeast Euroscarf GFP fusion collection and transformed into *pex3* and *pex3 atg1* cells, respectively. Subsequently, correct integration of *PEX14-mGFP* was confirmed by colony PCR using TER198 and TER199.

A fragment encoding 50bp flanking regions of *Pex14* and *mCherry* was cloned from plasmid pARM001 [29] using primers TER214 and TER215, and then transformed into BY4742 WT and *pex3 atg1* cells, respectively. Hygromycin resistant transformants were selected and correct integration was confirmed by colony PCR with primers TER216 and TER217. The *PEX8-mGFP* fragment was amplified with primers TER234 and TER235 using plasmid pMCE7 [30] as a template. A fragment encoding *mGFP-PEX8* under the control of the *NOP1* promoter (P_{NOP1}) was amplified with TER306 and TER307 using genomic DNA of strain AK259 as a template. *PEX10-mGFP*, *PEX11-mGFP*, *PEX13-mGFP*, *Ant1-mGFP* fragments were amplified from the yeast GFP fusion library with primers TER218 and TER219, TER222 and TER223, TER226 and TER227, TER299 and TER300, respectively. The above *PEX8-mGFP*, *PEX10*-mGFP, *PEX11*-mGFP, *PEX13-mGFP*, *Ant1-mGFP* fragments were transformed into BY4742 WT and *pex3 atgl* Pex14-mCherry cells. Correct integration was confirmed by colony PCR using the primers TER236/TER237, TER220/TER221, TER224/TER225, TER228/TER229, and TER301/TER302, respectively.

2.4.2 Construction of the *pex3 atg1* Pex14-mCherry query strain for Synthetic Genetic Array (SGA)—The *S. cerevisiae atg1 pex3* Pex14-mCherry query strain was constructed using an SGA compatible strain (yMS140). First *ATG1* was disrupted as described above. The PCR fragment was transformed into the SGA compatible strain and nourseothricin resistant transformants were checked by colony PCR using the primers JWR005 and JWR006, and confirmed by Southern blotting. A fragment encoding Pex14-mCherry was introduced in this strain as described before. *PEX3* was deleted by replacing the *PEX3* region with a cassette containing the zeocin resistance gene and 50 bp flanking regions of *PEX3.* The PCR fragment was amplified with the primers JWR051 and JWR052 using plasmid pSL34 as a template, and transformed into *atg1* Pex14-mCherry. Zeocin

resistant transformants were selected and the correct integration was checked by colony PCR using the primers TER202 and TER203 and confirmed by Southern blotting.

2.4.3 Construction of the CB199 *pex3 atg1* Pex14-TPA strain for biochemical studies—

For the generation of deletion mutant and genomically tagged protein strains, the corresponding cassettes were amplified from pUG27, pUG72 or pYM8 as previously described [31, 32]. Briefly, for tagging of the *PEX14* gene, the cassette *TEV-ProteinA-KanMX6* was amplified from plasmid pYM8 with the primers RE4354 and RE4355. For the deletion of the *PEX3* gene, the *HIS5* cassette was amplified from plasmid pUG27 with the primers RE4351 and RE4362. The clones were checked and selected by immunoblot analysis of Pex14 and Pex3. Finally, the *ATG1* gene was deleted using the *URA3* cassette amplified from plasmid pUG72 with primers RE4347 and RE4348. Mutant clones were selected and correct integration was checked by colony PCR using primers RE4349/RE4350 (Table S2).

2.5 Strain construction using the SGA method

The yMS140 *atg1 pex3* Pex14-mCherry query strain was crossed with strains containing N-terminal GFP-tagged peroxins of the SWAT-GFP library [33] using the SGA method [34, 35]. Mating was performed on rich media plates, and selection for diploid cells was performed on SD-URA plates containing Nourseothricin (200μg/ml). Sporulation was induced by transferring cells to nitrogen starvation media plates for 6 days. Haploid cells containing the *PEX3* and *ATG1* deletions, as well as Pex14-mCherry and one of the N-terminal GFP-tagged peroxins under control of the *NOP1* promoter were selected by transferring cells to SD-URA plates containing Nourseothricin (200μg/ml), Hygromycin B (200μg/ml) and Zeocin (200μg/ml) alongside the toxic amino acid derivatives Canavanine and Thialysine (Sigma-Aldrich) to select against remaining diploids, and lacking leucine to select for spores with an “alpha” mating type. The presence of the correct GFP fusion protein in the resulting *S. cerevisiae* strains was checked by colony PCR.

2.6 Generation of the*pex3 atgl* Pex14-mCherry Sur4-GFP strain

A *pex3 atg1* strain producing Pex14-mCherry and Sur3-GFP as an ER marker [36] was constructed by crossing *pex3 atg1* Pex14mCherry with a WT strain producing Sur4-GFP [37]. The correct strain was selected after sporulation.

2.7 Fluorescence and electron microscopy

To quantify Pex14-mGFP spots in *pex3* and *pex3 atg1* strains, cells were grown for 16h on MM-O. Random images were taken as a stack using a confocal microscope (LSM800, Carl Zeiss) and photomultiplier tubes (Hamamatsu Photonics) and Zen 2009 software (Carl Zeiss). Z-Stack images were made containing 14 optical slices and the GFP signal was visualized by excitation with a 488 nm argon ion laser (Lasos), and a 500-550 nm bandpass emission filter. Live cell imaging was performed using a Zeiss LSM800 confocal microscope. The temperature of the objective and object slide was kept at 30 °C and the cells were grown on 1% agar in medium. GFP fluorescence was analyzed by excitation of the cell with a 488 nm laser, and emission was detected using a 490-535 nm band-pass emission filter. DsRed fluorescence was analyzed by excitation with a 561 nm laser, and emission was

detected using a 535-700 nm band-pass filter. Eight z-axis planes were acquired every 20 min.

Fluorescence microscopy was performed by making single plain images for brightfield, mGFP and/or mCherry. All images were captured at room temperature using the AxioScope A1 microscope (Carl Zeiss), equipped with a 100x 1.30 NA Plan-Neofluar objective (Carl Zeiss), a digital camera (Coolsnap HQ2; Photometrics) and the Micro-Manager 1.4 software. Oleic acid grown cells were washed with water 2 times before image acquisition to remove oleic acid.

GFP fluorescence was visualized with a 470/40 nm band pass excitation filter, a 495 nm dichromatic mirror, and a 525/50 nm band-pass emission filter. mCherry fluorescence was visualized with a 587/25 nm band pass excitation filter, a 605 nm dichromatic mirror, and a 647/70 nm band-pass emission filter. Image analysis was carried out using ImageJ and Adobe Photoshop CS6 software.

Immuno-electron microscopy (immune-EM) and correlative light and electron microscopy (CLEM) was performed using cryosections as described previously [38]. The 6-nm gold particles that were used for immuno-EM were also used for alignment of the tomograms. For CLEM, sections were imaged on an Observer Z1 (Carl Zeiss) using Zen 2.3 software equipped with an AxioCAM MRm camera (Carl Zeiss) and a 63× 1.25 NA Plan-Neofluar objective (Carl Zeiss). GFP fluorescence was visualized with a 470/40-nm band pass excitation filter, a 495 nm dichromatic mirror, and a 525/50 nm band-pass emission filter. After fluorescence imaging, the grid was post-stained and embedded in a mixture of 0.5% uranyl acetate and 0.5% methylcellulose. Acquisition of the double-tilt tomography series for immuno-EM and CLEM was performed manually in a CM12 TEM running at 90 kV and included a tilt range of 40° to -40° with 2.5° increments. Reconstruction of the tomograms was performed using the IMOD software package. 3D surface-rendered models are generated using the AMIRA visualization package (TGS Europe).

2.8 Cell fractionation experiments

2.8.1 Subcellular fractionation and isopycnic density gradient cell fractionation—Cells were inoculated at an initial OD of 0.1 in 0.3% glucose media. After 8 h of cultivation, peroxisome proliferation was induced by adding oleic acid (0.1%). Postnuclear supernatants (PNS) were prepared as described previously [39]. Postnuclear supernatants derived from CB199 Pex14-TPA (considered from now on as WT), *pex3*, *atg1*, and *pex3 atg1* strains were loaded on a linear OptiPrep™ /sucrose gradient (2.24 to 36% (w/v) iodixanol gradient, containing 18% (w/v) sucrose). Centrifugation was performed with a TV-860 rotor [39].

2.8.2 Differential sedimentation—Postnuclear supernatants derived from WT, *pex3*, *atg1*, and *pex3 atg1* strains (1 ml) were applied onto a cushion of 200 µl 60% sucrose in lysis buffer [39]. The samples were centrifuged at 20,000 x g for 40 min in an MLA-130 rotor. The supernatants were loaded onto a new cushion and centrifuged at 200.000xg for 1 h 40 min. Samples were taken and proteins precipitated with TCA.

2.8.3 Flotation analysis—Postnuclear supernatants derived from WT, and *pex3 atg1* strains (15 ml) were applied onto a cushion of 5 ml 60% sucrose in lysis buffer (see above). The samples were centrifuged at 21,500 x g for 1 h 5 min in a Type Ti70 rotor. The supernatants were mixed with 50% OptiPrep™ /lysis buffer for a final concentration of 30% OptiPrep™ and 3 ml were applied to the bottom of the tube. Subsequently, 3ml of 25% OptiPrep™ /lysis buffer, 2 ml of 10% OptiPrep™ /lysis buffer, and 1.5 ml of lysis buffer were overlaid sequentially. The tubes were centrifuged at 90,000 x g for 14 h in an SW41 rotor. Fractions of 1 ml were taken for TCA precipitation.

2.9 Pex14-complex affinity purification

WT CB199 and *pex3 atg1* strains containing Pex14 genomically tagged with TEV (tobacco etch protease cleavage site)-ProteinA (TPA) were grown first in 0.3% glucose media and then oleic acid was added as described before. The cells were resuspended in lysis buffer (20 mM HEPES, 100 mM KOAc, and 5 mM MgOAc, pH 7.5) in the presence of protease inhibitors, disrupted with glass beads, and cell debris was sedimented at 1,500 x g for 10 min in an Eppendorf 5810R centrifuge. The membranes were sedimented for 1 h at 100,000 x g in a Sorvall T-647.5 rotor for 1 h. Sedimented membranes were resuspended and solubilized for 1 h 30 min in lysis buffer containing 1% digitonin (Calbiochem) at 3.3 mg/ml protein concentration. The solubilization of membrane proteins was followed by centrifugation for 1 h at 100,000 x g in a Sorvall T-647.5 rotor to remove not solubilized membrane proteins. The supernatants were incubated overnight in the presence of human IgG-Sepharose resin [40]. The complexes were eluted by digestion with TEV protease (Invitrogen) for 2 h at 16°C. For size-exclusion chromatography, eluted complexes from WT and *pex3 atg1* cells were applied to a Micro6Sepharose column pre-equilibrated with lysis buffer and 0.1% digitonin.

2.10 Quantitative LC-MS analysis of Pex14 complexes from the *pex3 atg1* strain

Pex14 complexes were affinity-purified from digitonin-solublized membranes of *pex3 atg1* cells expressing TPA-tagged or untagged (control) Pex14 in the CB199 background as described above in three independent replicates. Eluted proteins were precipitated with acetone, separated by SDS-PAGE using a 4-12% NuPAGE BisTris gradient gel (Life Technologies) and visualized by colloidal Coomassie Brilliant Blue. Gel lanes were cut into 22 equal slices each and processed for LC-MS analysis including reduction of disulfide bonds, subsequent alkylation of free thiol groups, and tryptic digestion essentially as described before [41]. LC-MS analyses were performed on an Orbitrap Elite mass spectrometer (Thermo Scientific, Bremen, Germany) coupled to an UltiMate 3000 RSLCnano HPLC system (ThermoScientific, Dreieich, Germany) as described previously [42].

Mass spectrometric raw data were processed using MaxQuant/Andromeda (version 1.5.2.8; [43] [44]). For protein identification, MS/MS data were searched against the *S. cerevisiae* Genome Database and a set of common contaminants provided by MaxQuant considering carbamidomethylation of cysteine residues as fixed and acetylation of protein N-termini and methionine oxidation as variable modifications. Proteins were identified with at least one unique peptide comprising a minimum of six amino acids and a false discovery rate of <

0.01 on peptide and protein level. Relative protein quantification was based on MS intensities determined by MaxQuant. Protein abundance ratios (Pex14-TPA/control) were calculated and mean log2 ratios across all three replicates as well as the p-value of each protein were determined using Perseus [45]. To be considered significantly enriched in Pex14 complexes, proteins were required to meet the following criteria: (i) identified in 3/3 Pex14-TPA purifications with at least 2 MS/MS counts in 2/3 replicates and (ii) identified in Pex14-TPA purifications only with a sequence coverage ≥ 20% or exhibiting a mean abundance ratio ≥ 5 (sequence coverage: ≥ 5%) and a p-value < 0.05. For details about proteins identified (sequence coverage ≥ 5%) and quantified, seeTable S3.

Results

3.1 Peroxisomal membrane remnants are present in *S. cerevisiae pex3* and *pex3 atg1* cells

The peroxisomal membrane structures observed in *H. polymorpha pex3* cells are sensitive to autophagic degradation, which could be blocked by deletion of *ATG1* [15]. Because this facilitated the detection of these structures in *H. polymorpha*, we also used an *atg1* background strain in order to address whether comparable structures are present in *S. cerevisiae pex3*. Fluorescence microscopy (FM) analysis of oleic acid-induced *pex3* and *pex3 atg1* cells producing Pex14-mGFP revealed the presence of distinct fluorescent spots (Fig. 1A). The average number of these spots was similar in *S. cerevisiae pex3* and *pex3 atg1* cells, as was evident from quantitative analysis of confocal laser scanning microscopy (CLSM) images (Fig. 1B). This result indicates that in *S. cerevisiae pex3* cells these structures are not, or at least not to the same extent as in *H. polymorpha,* subject to degradation by autophagy. This conclusion was supported by immunoblot analysis, which showed that the levels of Pex14 in *pex3* cells were the same as in wild-type (WT) and *pex3 atg1* cells (Fig. 1C). Further control experiments revealed that deletion of *ATG1* does not have a negative effect on peroxisome biogenesis or function, because *S. cerevisiae atg1* cells contain fully functional peroxisomes (normal growth on oleic acid), which show a similar sedimentation pattern as observed for WT controls (Fig. S1, compare Fig. 2B).

Because analysis of *S. cerevisiae pex3 atg1* cells allows precise comparison with data previously reported for *H. polymorpha pex3 atg1*, we continued our further studies with the double deletion strain.

Fluorescence microscopy revealed that the Pex14-mGFP spots were often closely associated to the ER in *S. cerevisiae pex3 atg1*, however, several spots can be observed that do not co-localize to the ER (Fig. 1D).

In order to further address the subcellular localization of Pex14-mGFP in *S. cerevisiae pex3 atg1* cells, we performed correlative light and electron microscopy (CLEM) in combination with tomography. As shown in Fig. 1E, electron tomography revealed that Pex14-GFP spots invariably represent clusters of vesicular structures. Although strands of ER were often present in the vicinity of these clusters, the CLEM studies never revealed the presence of GFP fluorescence at regions that only contained ER. Similarly, immunolabelling

experiments using α-Pex14 antibodies invariably showed labelling at vesicular structures (Fig. 1F), whereas labelling of the ER was never observed.

Summarizing, these data indicate that Pex14 is only present at clusters of vesicles in *S. cerevisiae pex3 atg1*. Although these vesicles sometimes appear in the vicinity of the ER, our detailed CLEM and immunolabelling experiments revealed that Pex14 is not localized at the ER in these cells.

Isopycnic density gradient cell fractionation showed that in *S. cerevisiae pex3 atg1* cells, most Pex14 protein co-migrated with the mitochondrial marker (Por1), together with a minor fraction that co-migrated with the ER marker (Kar2) (Fig. 2A). A similar distribution was observed in gradients of *pex3* control cells (Fig. S2). In contrast, in gradients of WT (Fig. 2A) or *atg1* (Fig. S2) control cells, virtually all Pex14 migrates to the bottom of the gradient (Fig 2A). In order to biochemically analyse the localization of Pex14 further, we performed sequential differential centrifugation. First, the postnuclear supernatants (PNS) prepared from the oleic acid induced WT and *pex3 atg1* cells were subjected to centrifugation for 40 min at 20, 000 x g (20 Kxg). This resulted in an almost complete sedimentation of the ER and mitochondria as indicated by the distribution of Por1 and Kar2 (Fig. 2B). In WT, the majority of Pex14 was in the 20 Kxg pellet fraction (P-20Kxg). However, in *pex3 atg1*, only a very small portion of Pex14 was found in the sediment, while the majority was observed in the corresponding supernatant (S-20Kxg). Subsequently, the S-20Kxg fraction was subjected to centrifugation at high speed (200 Kxg) in order to sediment small vesicles. After centrifugation, Pex14 was mostly present in the pellet (Fig. 2B). As expected, the peroxisomal matrix enzyme thiolase (Fox3) was mainly present in P-20Kxg of WT cells. However, this peroxisomal marker enzyme was observed in the P-20Kxg and P-200Kxg fractions of the *pex3 atg1* cells.

To analyze whether Pex14 is associated with membranes, we performed a flotation analysis of the supernatant of the 20Kxg sedimentation (Fig. 2C). Detection of Pex14 in fractions of lighter density in the *pex3 atg1* gradient indicated that it is associated with membranes. The Pex14 present in the WT S-20Kxg fraction did not float, indicating that Pex14 containing vesicles are not present in significant amounts in WT cells. The postnuclear supernatants (PNS) of both strains were also subjected to flotation analysis (Fig. 2D). As expected, the mitochondrial Por1 totally floated, as well as the ER protein Kar2, whereas the cytosolic enzyme Pgk1 remained at the loading point. The peroxisomal matrix protein Fox3 showed in gradient of the WT PNS a dual localization to peroxisomes and the cytosol as expected. Interestingly, in the absence of Pex3 a portion of Fox3 still floated.

These data suggest that *pex3 atg1* cells may harbor two populations of Pex14 containing vesicles: very small and empty ones in conjunction with larger ones that contain a minor portion of the cellular Fox3 protein. The larger ones sediment at 20 Kxg and also contain Fox3 (Fig. 2B). These vesicles are absent in the gradients of the S-20Kxg fraction (Fig. 2C), but float in the PNS gradients (Fig. 2D). The smaller ones sediment in the 200 Kxg fraction (Fig. 2B), but lack thiolase as is evident from the flotation gradient of the S-20Kxg fraction. The Fox3 protein which does not float in the PNS gradients may represent aggregates (Fig. 2D).

In order to address whether the Pex14-containing membrane structures in *S. cerevisiae pex3 atg1* cells have a similar protein composition as those observed in *H. polymorpha pex3 atg1* cells, we performed co-localization studies using Pex14-mCherry as peroxisome membrane-marker together with the same five PMPs that were tested in *H. polymorpha*, all C-terminally tagged with mGFP and under control of their endogenous promoters. As expected, the PMPs Pex10-mGFP, Pex11-mGFP, Pex13-mGFP and Ant1-mGFP were present in spots in WT control cells (Fig. 3A). However, part of Pex8-mGFP mislocalized to the cytosol in WT controls (Fig. 3A), which was not observed for a Pex8 variant, which was N-terminally tagged with mGFP, indicating that the C-terminal GFP tag influenced the localization of Pex8 to peroxisomes in WT cells.

In *S. cerevisiae pex3 atg1* cells, the bulk of the mGFP-Pex8 fluorescence also co-localized with Pex14-mCherry in spots (Fig. 3B), like in *H. polymorpha pex3 atg1*. However, Pex11-mGFP fluorescence was present at mitochondria (Fig. 3D), whereas Pex10-mGFP, Pex13-mGFP and Ant1-mGFP fluorescence was below the limit of detection (data not shown). The low levels of most PMPs was confirmed by western blot analysis of samples taken at different time points after a shift of *pex3 atg1* cells from glucose to oleic acid containing medium (Fig. 3C). Taken together, we conclude that Pex14 and Pex8 accumulate at membrane structures in *S. cerevisiae pex3 atg1* cells.

3.2 Several peroxins co-localize with Pex14 in *S. cerevisiae pex3 atg1* cells

In order to define a larger set of peroxins that co-localize with Pex14 in the absence of Pex3, additional localization studies were performed. Because in *pex3 atg1* cells the levels of several peroxins are extremely low (Fig. 3) when produced under control of the endogenous promoters (Fig. 3), we took advantage of the recently constructed SWAT-GFP library, which is a collection of ~2000 *S. cerevisiae* strains containing proteins tagged with GFP at the N-terminus and expressed using the constitutive *NOP1* promoter [33]. Using only the strains producing tagged peroxins from this library and synthetic genetic array (SGA), we obtained a collection of *pex3 atg1* double mutants producing Pex14-mCherry together with 19 different peroxins N-terminally tagged with mGFP. These proteins all (partially) localize to peroxisomes in WT cells, based on their co-localization with Pex3 [46].

As shown in Fig. 4 and Table 1, nine out of nineteen peroxins tested (partially) colocalized with Pex14-mCherry. The PTS1 receptor Pex5 and Pex7, but not the Pex7 co-receptors (Pex18 and Pex21) accumulate at the Pex14-mCherry spots (Fig. 4). Western blotting using anti-GFP antibodies revealed a band of approximately 34 kDa in cell extracts of GFP-Pex18 and GFP-Pex21 producing strains. Because both full length fusion proteins have a calculated molecular weight of approximately 60 kDa, this result indicates that these fusion proteins are most likely proteolytically cleaved (Fig. 5; see Table 1 for calculated MW of the fusion proteins). The docking proteins (Pex13, Pex17) and Pex8 colocalized with Pex14-mCherry. Of these peroxins, Pex17 showed relatively high levels of a 34 kDa band that is recognized by the anti-GFP antibodies and may explain the partial cytosolic fluorescence in the double mutant cells (Fig. 4). Pex4 and its recruiting protein Pex22 were also present at the Pex14 spots. None of the three RING proteins co-localized with Pex14. Western blotting indicated that a significant portion of GFP-Pex2 and most of the GFP-Pex10 and GFP-Pex12 was

cleaved. GFP-Pex15, which was only partially cleaved, also partially co-localized with Pex14-mCherry. Both AAA peroxins Pex1 and Pex6 as well as Pex19 were observed in the cytosol. Finally, of the three proteins of the Pex11 family (Pex11, Pex25, Pex27), Pex11 localized to mitochondria, Pex25 localized both to Pex14 spots and the cytosol, whereas Pex27 was exclusively localized to the cytosol. However, for Pex27 only the cleaved protein was detected in the western blot (Fig. 5). Western blot analysis of WT control strains overproducing the same N-terminally tagged fusion proteins revealed that for all peroxins the full length protein was detectable, although some of the peroxins showed significant levels of cleaved protein as well. Major differences were observed for Pex10, Pex25 and Pex27, which were present almost exclusively at full length in WT, in contrast to *atg1 pex3* cells in which these proteins were almost completely cleaved.

3.3 Pex14 forms a complex with other peroxins in *pex3 atg1* cells

In a complementary approach, Pex14 was genomically tagged with protein A (TPA-tag) and Pex14-containing complexes were isolated from WT and *pex3 atg1* mutant cells and compared regarding their size and composition (Fig. 6A). Like the Pex14-mGFP fusion protein, Protein A-tagged Pex14 is fully functional (Fig. S1). In WT, two main complexes were detected. One of about 700 kDa that corresponds well to the known complex with Pex14-Pex13-Pex17-Pex5 as major constituents, which was described earlier as the PTS1 import pore [47]. The second complex also contains the components of the PTS1 import pore but migrates to fractions representing structures of higher molecular weight. Interestingly, the higher molecular weight complex is not observed in the *pex3 atg1* double mutant. The composition of the isolated Pex14 complexes from *pex3 atg1* cells was also analyzed by quantitative mass spectrometry. In addition to Pex14, Pex13, Pex17, and Pex5 as detected by immunoblot analysis, the PTS2-receptor Pex7 and its co-receptor Pex18, Pex4, Pex22, and Pex25 were also part of the complex (Fig. 6B). Moreover, non-peroxisomal proteins were also found to be enriched with Pex14-TPA, mainly from the cytosol, ER, and Golgi (Fig. 6C). The results are in good agreement with the fluorescence microscopy data, with the exception that Pex8 and Pex15 were not detected in the complex by biochemical means. This indicates that although Pex8 and Pex15 co-localized with Pex14 in membrane vesicles, they apparently did not associated to the large Pex14-containing protein complex.

4 Discussion

Here we show that in *S. cerevisiae pex3 atg1* cells PMPs do not accumulate at the ER. Our fluorescence microscopy data, supported by electron microscopy and biochemical analyses, revealed that Pex14 localizes to membrane vesicles, which are morphologically distinct from the ER and do not co-sediment with ER markers in cell fractionation experiments. At these vesicles, Pex14 assembles with other peroxins to form a complex with a composition similar to the PTS1 pore in WT cells [47].

The peroxisomal membrane structures observed in *S. cerevisiae pex3 atg1* cells are similar to those described in *H. polymorpha pex3 atg1*, because they also contain Pex8, Pex13 and Pex14, but not Pex10, Pex11 or Ant1 (Figs. 2 and 4). However, in *S. cerevisiae pex3* these

structures are relatively stable, whereas in *H. polymorpha pex3* they are subject to constitutive autophagic degradation [15]. This can readily be explained by the difference in function of Pex3 in pexophagy in these two yeast species. In *S. cerevisiae* Pex3 is required for pexophagy, because it recruits Atg36 [48]. Hence, in the absence of Pex3 peroxisomal structures will not be recognized by the autophagy machinery. In contrast, in *H. polymorpha* Pex3 should be first removed from peroxisomes to allow pexophagy [49, 50]. Cells of *ATG1* single deletion strains have increased peroxisome numbers both in *H. polymorpha* [51] and *S. cerevisiae* [52], which can be explained by low levels of constitutive autophagy.

Of the 19 additional peroxins tested, 9 (partially) co-localized with Pex14 (Table 1). Based on these co-localization experiments together with the proteomic analysis of Pex14 complexes, we conclude that *S. cerevisiae pex3* cells contain peroxisomal membrane vesicles, which harbor a receptor docking complex, PTS receptors and a large protein complex with the same composition as the matrix protein import pore in WT cells. This import pore is most likely also functional, because the structures contain small amounts of the matrix enzyme thiolase (Fig. 2D). In this respect, the vesicles also resemble those present in *H. polymorpha pex3 atg1* cells, which harbor small amounts of the peroxisomal matrix protein alcohol oxidase.

Recycling of the PTS receptors involves ubiquitination processes by the E2 enzyme Pex4, which is recruited to peroxisomes by the PMP Pex22, together with the three RING peroxins, which serve as E3 enzymes. Pex4-GFP and Pex22-GFP co-localize with Pex14-mCherry to the vesicles and were detected in the Pex14 complexes, but not the RING proteins, most likely explaining why Pex5 and Pex7 accumulate at the structures.

Because of the absence of a functional exportomer matrix protein import cannot proceed when all receptor molecules have accumulated at the docking/import site. This may explain why there is only little import of thiolase. The absence of the RING proteins in the structures most likely also prevents the formation of the entire importomer, which is indicated by the lack of a high molecular weight Pex14 complex in *pex3* cells.

The final steps in receptor recycling require the AAA ATPases Pex1 and Pex6. GFP-Pex1 and GFP-Pex6 fluorescence was relatively strong and present in the cytosol. However, the Pex1/Pex6 recruiting protein Pex15 did co-localize to the Pex14-containing vesicles. The cytosolic localization of Pex1/Pex6 may be due to the fact that upon overproduction these proteins cannot fully assemble in Pex1/Pex6/Pex15 complexes [53]. The lack of Pex15 in the isolated Pex14-complex might be caused by the absence of Pex3 or the RING-complex bridging the pore and the AAA-complex.

Several PMPs did not accumulate at the membrane vesicles, e.g. Pex11 accumulated at mitochondria in line with earlier reports [14, 54]. In *H. polymorpha pex3*, Pex11 was observed at the ER in the transient stage of adapting cells to methanol growth conditions. This difference in Pex11 location in the two yeast species supports the view that Pex11 mislocalizes in the absence of Pex3. We also observed a significantly reduced Pex11 level in the *S. cerevisiae* cells lacking Pex3, relative to the WT control, suggesting that the protein is not very stable at mitochondria (Fig. 2C). Of the two other proteins of the Pex11 family,

Pex25 and Pex27, only Pex25 co-localized with Pex14 and was detected in the Pex14 complex by MS, whereas Pex27 appeared to be relatively unstable.

The sorting mechanisms of PMPs are still debated. According to the classical model, most PMPs (class 1) are recognized by the mPTS receptor Pex19, which is recruited to the peroxisome by Pex3, followed by insertion of the cargo PMP via a yet unknown mechanism. Pex3 itself is a class 2 protein and inserts into peroxisomal membranes independent of this machinery. For Pex3, the targeting signal resides in the extreme N-terminus. Pex3 shares a similar N-terminal domain responsible for intracellular trafficking with Pex22 [55, 56]. When the N-terminal fragment of Pex3 was replaced by the corresponding fragment of Pex22, the protein was targeted to functional peroxisomes [55]. As Pex22 and Pex3 follow the same import route, the presence of Pex22 in the membrane vesicles in *pex3* cells supports the view that also this protein sorts to the peroxisomal membrane independent of Pex3. Pex8 is a peroxisomal matrix protein that only requires PTS receptors and Pex14 for import [57, 58]. This peroxin also associates to the peroxisomal vesicles stressing the presence of a functional matrix protein import pore. However, it remains unclear how the other PMPs sort to the vesicles in *pex3* cells because they are assumed to be class 1 proteins and hence require Pex3 and Pex19 for sorting to peroxisomes (Pex13, Pex14, Pex15, Pex17, Pex15, Pex22 and Pex25).

According to an alternative PMP sorting pathway, proposed by van der Zand and colleagues [4, 10], all PMPs first insert in the ER and exit this compartment in Pex3/Pex19 dependent way. Our observations are not consistent with this model, because it predicts that all PMPs accumulate at the ER in the absence of Pex3. One option could be that PMPs indeed first sort to the ER, but that vesicle formation is not strictly dependent on Pex3. However, in that case all PMPs, and not only a subset, should be localized to the membrane vesicles. Interestingly, recent studies in the yeast *Pichia pastoris* suggested that the RING proteins Pex2, Pex10 and Pex12, but not proteins of the docking complex (Pex13, Pex14, Pex17) require Pex3 for intra-ER sorting and packaging in ER-derived vesicles [59]. Consequently, the RING proteins accumulate at the ER in *P. pastoris pex3* cells. Based on our fluorescence microscopy, cell fractionation and proteomics studies the RING proteins do not accumulate at the ER in *S. cerevisiae pex3* cells.

A major open question remains how the peroxisomal membrane vesicles are formed in *pex3* cells. We envisage two possible options. One includes that a subset of the PMPs travel via the ER followed by Pex3-independent enclosure in ER-derived vesicles. In this scenario, the PMPs that do not follow this pathway (e.g. the RING proteins, Pex11 and Pex27) are mistargeted. A second option is that the membrane structures are semi-autonomous and proliferate via growth and fission. In this view a subset of the PMPs directly sort to the membranes via a yet unknown, Pex3 independent mechanism, while others do require Pex3 for correct sorting. Additional research is required in order to solve this important question.

Supplementary Material

Refer to Web version on PubMed Central for supplementary material.

Europe PMC Funders Author Manuscripts

Acknowledgements

We are grateful to Kevin Knoops and Arjen M. Krikken for their assistance in various parts of the work. Funding: This work was supported by grants from Marie Curie Initial Training Networks (ITN) program PerFuMe (Grant Agreement Number 316723) to J.P.W. and L.D.C.Z, the CHINA SCHOLARSHIP COUNCIL to Y.W., an ERC CoG Peroxisystem 646604 to M.S. and E.Z., the Deutsche Forschungsgemeinschaft (FOR 1905 to B.W., and R.E.; RTG 2202 to B.W.) and the Excellence Initiative of the German Federal & State Governments (EXC 294 BIOSS to BW). The authors declare no competing financial interests.

References

[1]. Smith JJ, Aitchison JD. Peroxisomes take shape, Nature reviews. Molecular cell biology. 2013; 14:803–817. [PubMed: 24263361]

[2]. Mast FD, Rachubinski RA, Aitchison JD. Signaling dynamics and peroxisomes. Current opinion in cell biology. 2015; 35:131–136. [PubMed: 26042681]

[3]. Schrader M, Costello JL, Godinho LF, Azadi AS, Islinger M. Proliferation and fission of peroxisomes – An update. Biochimica et biophysica acta. 2016; 1863:971–983. [PubMed: 26409486]

[4]. Hoepfner D, Schildknegt D, Braakman I, Philippsen P, Tabak HF. Contribution of the endoplasmic reticulum to peroxisome formation. Cell. 2005; 122:85–95. [PubMed: 16009135]

[5]. Tabak HF, Braakman I, van der Zand A. Peroxisome Formation and Maintenance Are Dependent on the Endoplasmic Reticulum. Annual review of biochemistry. 2013

[6]. Agrawal G, Subramani S. De novo peroxisome biogenesis: Evolving concepts and conundrums. Biochimica et biophysica acta. 2015

[7]. Lam SK, Yoda N, Schekman R. A vesicle carrier that mediates peroxisome protein traffic from the endoplasmic reticulum. Proceedings of the National Academy of Sciences of the United States of America. 2011; 108:E51–52. [PubMed: 21467226]

[8]. Agrawal G, Joshi S, Subramani S. Cell-free sorting of peroxisomal membrane proteins from the endoplasmic reticulum. Proceedings of the National Academy of Sciences of the United States of America. 2011; 108:9113–9118. [PubMed: 21576455]

[9]. Hettema EH, Girzalsky W, van Den Berg M, Erdmann R, Distel B. Saccharomyces cerevisiae pex3p and pex19p are required for proper localization and stability of peroxisomal membrane proteins. The EMBO journal. 2000; 19:223–233. [PubMed: 10637226]

[10]. van der Zand A, Braakman I, Tabak HF. Peroxisomal membrane proteins insert into the endoplasmic reticulum. Molecular biology of the cell. 2010; 21:2057–2065. [PubMed: 20427571]

[11]. van der Zand A, Gent J, Braakman I, Tabak HF. Biochemically distinct vesicles from the endoplasmic reticulum fuse to form peroxisomes. Cell. 2012; 149:397–409. [PubMed: 22500805]

[12]. Stroobants AK, Hettema EH, van den Berg M, Tabak HF. Enlargement of the endoplasmic reticulum membrane in Saccharomyces cerevisiae is not necessarily linked to the unfolded protein response via Ire1p. FEBS letters. 1999; 453:210–214. [PubMed: 10403405]

[13]. Mattiazzi Usaj M, Brloznik M, Kaferle P, Zitnik M, Wolinski H, Leitner F, Kohlwein SD, Zupan B, Petrovic U. Genome-Wide Localization Study of Yeast Pex11 Identifies PeroxisomeMitochondria Interactions through the ERMES Complex. Journal of molecular biology. 2015

[14]. Motley AM, Galvin PC, Ekal L, Nuttall JM, Hettema EH. Reevaluation of the role of Pex1 and dynamin-related proteins in peroxisome membrane biogenesis. The Journal of cell biology. 2015; 211:1041–1056. [PubMed: 26644516]

[15]. Knoops K, Manivannan S, Cepinska MN, Krikken AM, Kram AM, Veenhuis M, van der Klei IJ. Preperoxisomal vesicles can form in the absence of Pex3. The Journal of cell biology. 2014; 204:659–668. [PubMed: 24590171]

[16]. van der Klei I, Veenhuis M, van der Ley I, Harder W. Heterologous expression of alcohol oxidase in Saccharomyces cerevisiae: properties of the enzyme and implications for microbody development. FEMS microbiology letters. 1989; 48:133–137. [PubMed: 2656378]

[17]. Baerends RJ, Faber KN, Kram AM, Kiel JA, van der Klei IJ, Veenhuis M. A stretch of positively charged amino acids at the N terminus of Hansenula polymorpha Pex3p is involved in incorporation of the protein into the peroxisomal membrane. The Journal of biological chemistry. 2000; 275:9986–9995. [PubMed: 10744674]

[18]. Hohfeld J, Veenhuis M, Kunau WH. PAS3, a Saccharomyces cerevisiae gene encoding a peroxisomal integral membrane protein essential for peroxisome biogenesis. The Journal of cell biology. 1991; 114:1167–1178. [PubMed: 1894692]

[19]. Albertini M, Rehling P, Erdmann R, Girzalsky W, Kiel JA, Veenhuis M, Kunau WH. Pex14p, a peroxisomal membrane protein binding both receptors of the two PTS-dependent import pathways. Cell. 1997; 89:83–92. [PubMed: 9094717]

[20]. Erdmann R, Blobel G. Giant peroxisomes in oleic acid-induced Saccharomyces cerevisiae lacking the peroxisomal membrane protein Pmp27p. The Journal of cell biology. 1995; 128:509–523. [PubMed: 7860627]

[21]. Girzalsky W, Rehling P, Stein K, Kipper J, Blank L, Kunau WH, Erdmann R. Involvement of Pex13p in Pex14p localization and peroxisomal targeting signal 2-dependent protein import into peroxisomes. The Journal of cell biology. 1999; 144:1151–1162. [PubMed: 10087260]

[22]. Huhse B, Rehling P, Albertini M, Blank L, Meller K, Kunau WH. Pex17p of Saccharomyces cerevisiae is a novel peroxin and component of the peroxisomal protein translocation machinery. The Journal of cell biology. 1998; 140:49–60. [PubMed: 9425153]

[23]. Erdmann R, Kunau WH. Purification and immunolocalization of the peroxisomal 3-oxoacyl-CoA thiolase from Saccharomyces cerevisiae. Yeast. 1994; 10:1173–1182. [PubMed: 7754706]

[24]. Kerssen D, Hambruch E, Klaas W, Platta HW, de Kruijff B, Erdmann R, Kunau WH, Schliebs W. Membrane association of the cycling peroxisome import receptor Pex5p. The Journal of biological chemistry. 2006; 281:27003–27015. [PubMed: 16849337]

[25]. Rose MD, Misra LM, Vogel JP. KAR2, a karyogamy gene, is the yeast homolog of the mammalian BiP/GRP78 gene. Cell. 1989; 57:1211–1221. [PubMed: 2661018]

[26]. Truscott KN, Kovermann P, Geissler A, Merlin A, Meijer M, Driessen AJ, Rassow J, Pfanner N, Wagner R. A presequence- and voltage-sensitive channel of the mitochondrial preprotein translocase formed by Tim23. Nature structural biology. 2001; 8:1074–1082. [PubMed: 11713477]

[27]. Ozimek P, van Dijk R, Latchev K, Gancedo C, Wang DY, van der Klei IJ, Veenhuis M. Pyruvate carboxylase is an essential protein in the assembly of yeast peroxisomal oligomeric alcohol oxidase. Molecular biology of the cell. 2003; 14:786–797. [PubMed: 12589070]

[28]. Goldstein AL, McCusker JH. Three new dominant drug resistance cassettes for gene disruption in Saccharomyces cerevisiae. Yeast. 1999; 15:1541–1553. [PubMed: 10514571]

[29]. Kumar S, Singh R, Williams CP, van der Klei IJ. Stress exposure results in increased peroxisomal levels of yeast Pnc1 and Gpd1, which are imported via a piggy-backing mechanism. Biochimica et biophysica acta. 2016; 1863:148–156. [PubMed: 26516056]

[30]. Cepinska MN, Veenhuis M, van der Klei IJ, Nagotu S. Peroxisome fission is associated with reorganization of specific membrane proteins. Traffic. 2011; 12:925–937. [PubMed: 21507161]

[31]. Gueldener U, Heinisch J, Koehler GJ, Voss D, Hegemann JH. A second set of loxP marker cassettes for Cre-mediated multiple gene knockouts in budding yeast. Nucleic Acids Research. 2002; 30 e23 [PubMed: 11884642]

[32]. Knop M, Siegers K, Pereira G, Zachariae W, Winsor B, Nasmyth K, Schiebel E. Epitope tagging of yeast genes using a PCR-based strategy: more tags and improved practical routines. Yeast. 1999; 15:963–972. [PubMed: 10407276]

[33]. Yofe I, Weill U, Meurer M, Chuartzman S, Zalckvar E, Goldman O, Ben-Dor S, Schutze C, Wiedemann N, Knop M, Khmelinskii A, et al. One library to make them all: streamlining the creation of yeast libraries via a SWAp-Tag strategy. Nature methods. 2016; 13:371–378. [PubMed: 26928762]

[34]. Tong AH, Boone C. Synthetic genetic array analysis in Saccharomyces cerevisiae. Methods Mol Biol. 2006; 313:171–192. [PubMed: 16118434]

[35]. Cohen Y, Schuldiner M. Advanced methods for high-throughput microscopy screening of genetically modified yeast libraries. Methods Mol Biol. 2011; 781:127–159. [PubMed: 21877281]

[36]. David D, Sundararabu S, Gerst JE. Involvement of long chain fatty acid elongation in the trafficking of secretory vesicles in yeast. The Journal of cell biology. 1998; 143:1167–1182. [PubMed: 9832547]

[37]. Huh WK, Falvo JV, Gerke LC, Carroll AS, Howson RW, Weissman JS, O'Shea EK. Global analysis of protein localization in budding yeast. Nature. 2003; 425:686–691. [PubMed: 14562095]

[38]. Knoops K, de Boer R, Kram A, van der Klei IJ. Yeast pex1 cells contain peroxisomal ghosts that import matrix proteins upon reintroduction of Pex1. The Journal of cell biology. 2015; 211:955–962. [PubMed: 26644511]

[39]. Cramer J, Effelsberg D, Girzalsky W, Erdmann R. Isolation of Peroxisomes from Yeast. Cold Spring Harbor protocols. 2015; 2015 pdb top074500 [PubMed: 26330630]

[40]. Agne B, Meindl NM, Niederhoff K, Einwachter H, Rehling P, Sickmann A, Meyer HE, Girzalsky W, Kunau WH. Pex8p: an intraperoxisomal organizer of the peroxisomal import machinery. Molecular cell. 2003; 11:635–646. [PubMed: 12667447]

[41]. Cristodero M, Mani J, Oeljeklaus S, Aeberhard L, Hashimi H, Ramrath DJ, Lukes J, Warscheid B, Schneider A. Mitochondrial translation factors of Trypanosoma brucei: elongation factor-Tu has a unique subdomain that is essential for its function. Molecular microbiology. 2013; 90:744–755. [PubMed: 24033548]

[42]. Hunten S, Kaller M, Drepper F, Oeljeklaus S, Bonfert T, Erhard F, Dueck A, Eichner N, Friedel CC, Meister G, Zimmer R, et al. p53-Regulated Networks of Protein, mRNA, miRNA, and lncRNA Expression Revealed by Integrated Pulsed Stable Isotope Labeling With Amino Acids in Cell Culture (pSILAC) and Next Generation Sequencing (NGS) Analyses. Molecular & cellular proteomics : MCP. 2015; 14:2609–2629. [PubMed: 26183718]

[43]. Cox J, Mann M. MaxQuant enables high peptide identification rates, individualized p.p.b.-range mass accuracies and proteome-wide protein quantification. Nature biotechnology. 2008; 26:1367–1372.

[44]. Cox J, Neuhauser N, Michalski A, Scheltema RA, Olsen JV, Mann M. Andromeda: a peptide search engine integrated into the MaxQuant environment. Journal of proteome research. 2011; 10:1794–1805. [PubMed: 21254760]

[45]. Tyanova S, Temu T, Sinitcyn P, Carlson A, Hein MY, Geiger T, Mann M, Cox J. The Perseus computational platform for comprehensive analysis of (prote)omics data. Nature methods. 2016

[46]. Yifrach E, Chuartzman SG, Dahan N, Maskit S, Zada L, Weill U, Yofe I, Olender T, Schuldiner M, Zalckvar E. Characterization of proteome dynamics in oleate reveals a novel peroxisome targeting receptor. Journal of cell science. 2016

[47]. Meinecke M, Cizmowski C, Schliebs W, Kruger V, Beck S, Wagner R, Erdmann R. The peroxisomal importomer constitutes a large and highly dynamic pore. Nature cell biology. 2010; 12:273–277. [PubMed: 20154681]

[48]. Motley AM, Nuttall JM, Hettema EH. Pex3-anchored Atg36 tags peroxisomes for degradation in Saccharomyces cerevisiae. The EMBO journal. 2012; 31:2852–2868. [PubMed: 22643220]

[49]. Bellu AR, Salomons FA, Kiel JA, Veenhuis M, Van Der Klei IJ. Removal of Pex3p is an important initial stage in selective peroxisome degradation in Hansenula polymorpha. The Journal of biological chemistry. 2002; 277:42875–42880. [PubMed: 12221086]

[50]. Zutphen T, Veenhuis M, van der Klei IJ. Pex14 is the sole component of the peroxisomal translocon that is required for pexophagy. Autophagy. 2008; 4:63–66. [PubMed: 17921697]

[51]. Aksam EB, Koek A, Kiel JA, Jourdan S, Veenhuis M, van der Klei IJ. A peroxisomal lon protease and peroxisome degradation by autophagy play key roles in vitality of Hansenula polymorpha cells. Autophagy. 2007; 3:96–105. [PubMed: 17172804]

[52]. Reggiori F, Monastyrska I, Shintani T, Klionsky DJ. The actin cytoskeleton is required for selective types of autophagy, but not nonspecific autophagy, in the yeast Saccharomyces cerevisiae. Molecular biology of the cell. 2005; 16:5843–5856. [PubMed: 16221887]

[53]. Rosenkranz K, Birschmann I, Grunau S, Girzalsky W, Kunau WH, Erdmann R. Functional association of the AAA complex and the peroxisomal importomer. The FEBS journal. 2006; 273:3804–3815. [PubMed: 16911527]

[54]. MattiazziUsaj M, Brloznik M, Kaferle P, Zitnik M, Wolinski H, Leitner F, Kohlwein SD, Zupan B, Petrovic U. Genome-Wide Localization Study of Yeast Pex11 Identifies Peroxisome-Mitochondria Interactions through the ERMES Complex. Journal of molecular biology. 2015; 427:2072–2087. [PubMed: 25769804]

[55]. Halbach A, Rucktaschel R, Rottensteiner H, Erdmann R. The N-domain of Pex22p can functionally replace the Pex3p N-domain in targeting and peroxisome formation. The Journal of biological chemistry. 2009; 284:3906–3916. [PubMed: 19017643]

[56]. Fakieh MH, Drake PJ, Lacey J, Munck JM, Motley AM, Hettema EH. Intra-ER sorting of the peroxisomal membrane protein Pex3 relies on its luminal domain. Biology open. 2013; 2:829–837. [PubMed: 23951409]

[57]. Zhang L, Leon S, Subramani S. Two independent pathways traffic the intraperoxisomal peroxin PpPex8p into peroxisomes: mechanism and evolutionary implications. Molecular biology of the cell. 2006; 17:690–699. [PubMed: 16319171]

[58]. Ma C, Schumann U, Rayapuram N, Subramani S. The peroxisomal matrix import of Pex8p requires only PTS receptors and Pex14p. Molecular biology of the cell. 2009; 20:3680–3689. [PubMed: 19570913]

[59]. Agrawal G, Fassas SN, Xia ZJ, Subramani S. Distinct requirements for intra-ER sorting and budding of peroxisomal membrane proteins from the ER. The Journal of cell biology. 2016; 212:335–348. [PubMed: 26833788]

Europe PMC Funders Author Manuscripts

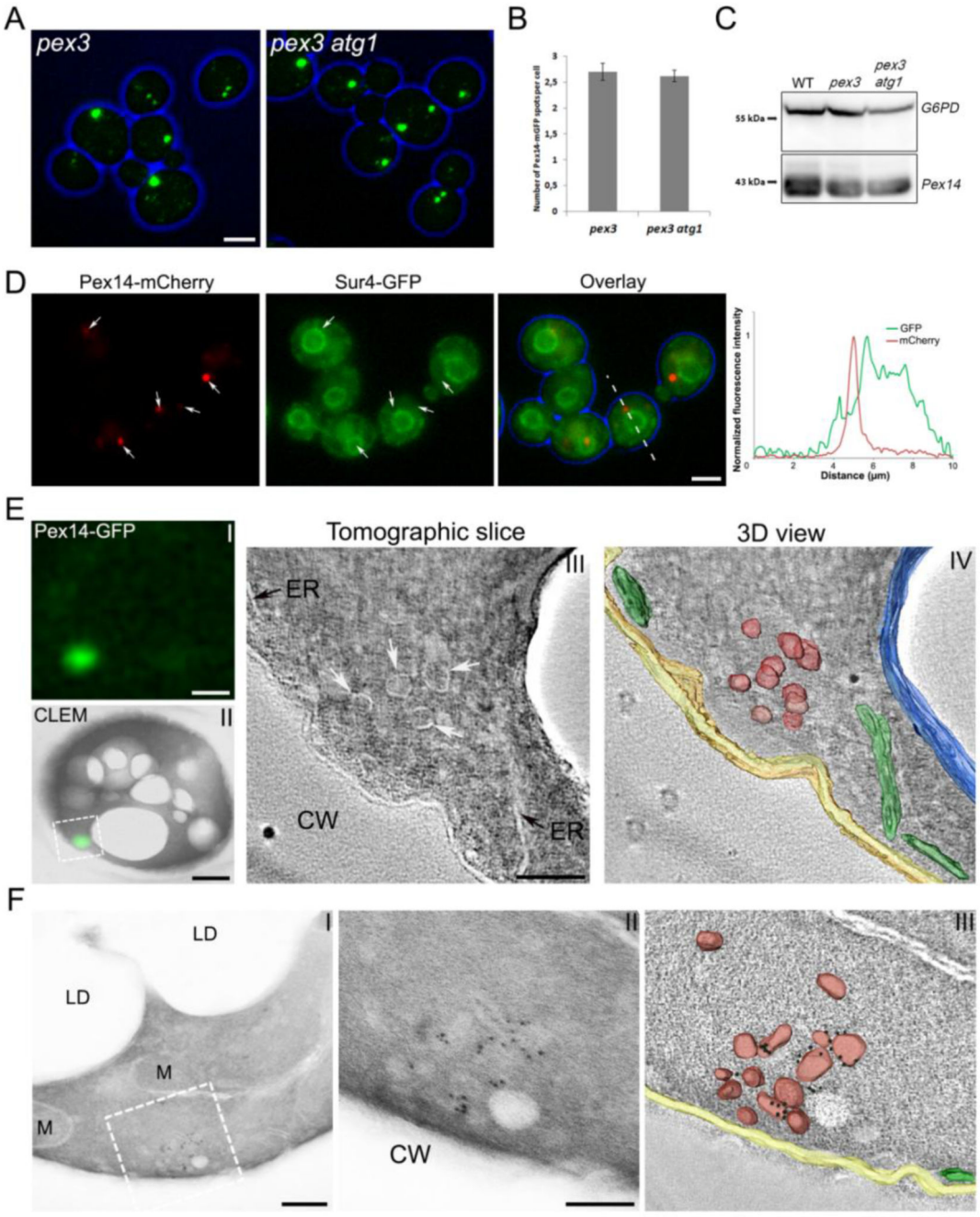

Figure 1. Peroxisomal membrane structures are present in *S. cerevisiae pex3* and *pex3 atg1* cells.
Cells were grown on MM-O for 16 h. (**A**) FM images of *pex3* and *pex3 atg1* cells producing Pex14-mGFP. Scale bar: 2.5 μm. (**B**) Quantification of Pex14-mGFP spots in *pex3* and *pex3 atg1* cells. The average number of spots was calculated from 250 cells in each strain. Error bars represent standard deviation (SD) of two independent experiments. (**C**) Western blot analysis of Pex14 levels in WT, *pex3* and *pex3 atg1* cells. Glucose 6 phosphate dehydrogenase (G6PD) was used as loading control. (**D**) FM images of *pex3 atg1* cells producing Pex14-mCherry and Sur4-GFP as the ER marker. Graphs show normalized

fluorescence intensities along the lines indicated in the merged image. The peak of highest intensity was set to 1. (**E**) CLEM of *pex3 atg1* cells producing Pex14-GFP. I) The localization of Pex14-GFP in a 160 nm thick cryosection using FM. II) Overlay of the same FM image together with the EM image. III) A tomographic slice of the region boxed in (II), where the fluorescent spot is localized. IV) 3D rendered volume showing peroxisomal vesicles (red), ER (green), vacuolar membrane (blue) and plasma membrane (yellow). **F** I) Immuno-EM of *pex3 atg1* cell using a 90nm thick cryosection and anti-Pex14 antibodies. II) Higher magnification of the region indicated in I. III) 3D view of the tomogram of the image shown in (II), indicating the peroxisomal vesicles (red), ER (green), plasma membrane (yellow) and 6nm gold particles (black). Scale bars (E I, II) 500nm; (E III) 100nm; (F I) 200nm; (F II) 100nm. CW – cell wall, LD – lipid droplet, M – mitochondrion.

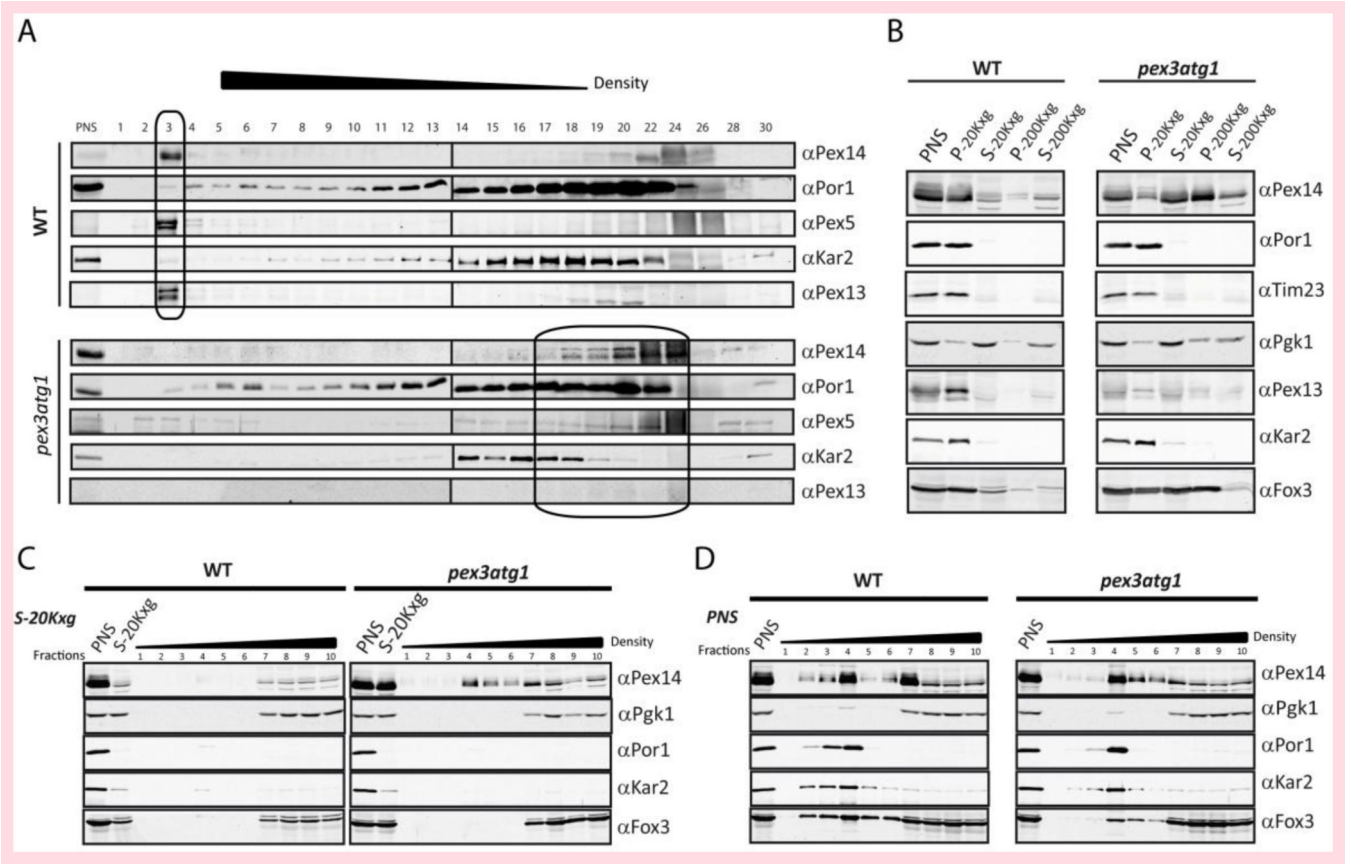

Figure 2. Pex14 is localized to membrane structures in the absence of Pex3.

(**A**) Cells were grown in the presence of oleic acid. Postnuclear supernatants (PNS) from WT and *pex3 atg1* double mutant cells were fractionated by isopycnic density gradient centrifugation. Fractions were analyzed by immunoblotting with antibodies against Pex14, Pex5 and Pex13 (peroxisomes), Kar2 (ER) and Por1 (mitochondria). Pex14-containing fractions are indicated by a box. (**B**) Separation of organelles by differential centrifugation. PNS were generated and sequentially centrifuged at 20,000 x g for 40 min (20Kxg) and then at 200,000 x g for 1 h 40 min (200Kxg). Fractions were analyzed by immunoblotting using antibodies against Por1 and Tim23 (mitochondria); Kar2 (ER); 3-phosphoglycerate kinase (Pgk1, cytosol); Pex14, Pex13 and thiolase (Fox3) (peroxisomes). Flotation analysis of the 20Kxg supernatant (**C**) or PNS (**D**) of WT and *pex3 atg1* cells.

Europe PMC Funders Author Manuscripts

Europe PMC Funders Author Manuscripts

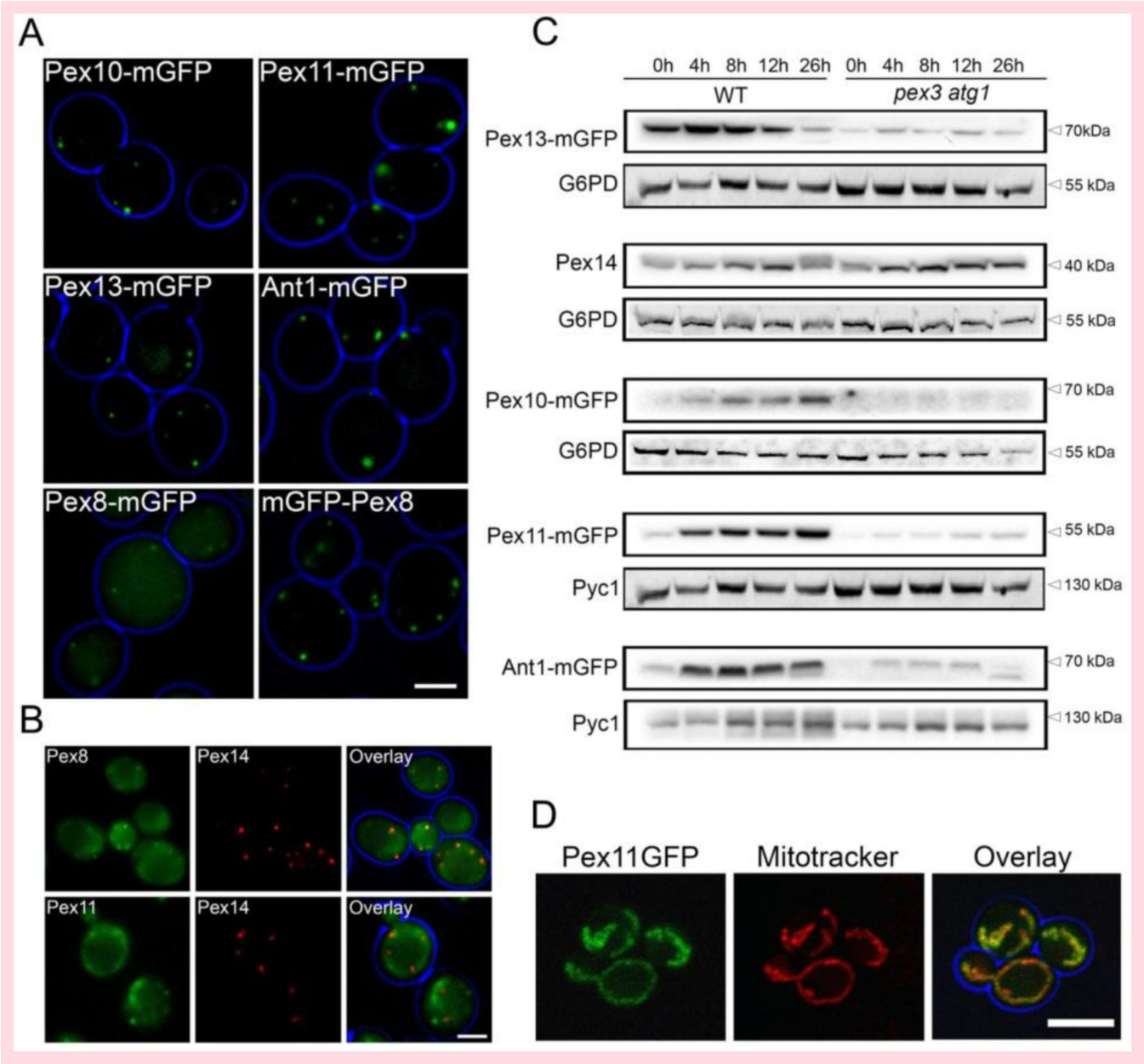

Figure 3. PMPs levels and localization in WT and *pex3 atg1* cells.

FM analysis of glucose-grown WT (**A**) or *pex3 atg1* cells (**B**) producing various C-terminal GFP-tagged PMPs under control of their endogenous promoters. mGFP-Pex8 was produced under control of P_{NOP1}. The *pex3 atg1* cells (**B**) also produce Pex14-mCherry to mark the peroxisomal vesicles. **(C**) Western blot analysis of the indicated GFP fusion proteins (produced under control of their endogenous promoters) in whole cell lysates of WT and *pex3 atg1* cells. Cells were pre-cultivated in minimal media containing glucose, subsequently shifted to media containing a mixture of glucose and oleic acid. Samples were taken at the indicated time points after the shift. Pyc1 or G6PD were used as loading controls. (**D**) Confocal laser scanning microscopy analysis of *pex3 atg1* cells producing Pex11-mGFP under control of the P_{PEX11}. Mitochondria were stained with Mitotracker

(Red). Living cells growing on glucose medium containing 1% agar were imaged. Scale bars: 2.5 μm (A), 5 μm (B, D).

Europe PMC Funders Author Manuscripts

Europe PMC Funders Author Manuscripts

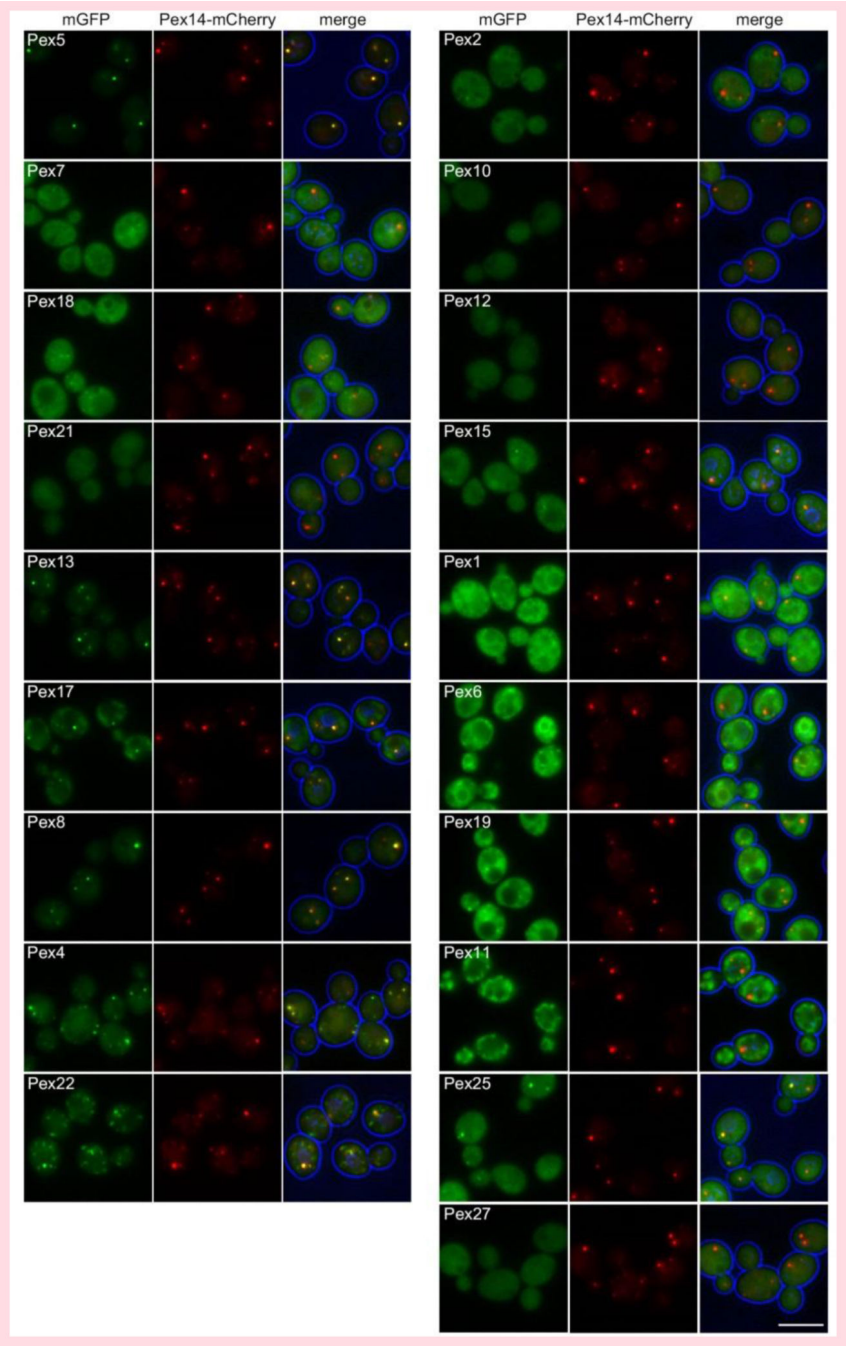

Figure 4. Localization of peroxins in *S. cerevisiae pex3 atg1* double mutant cells.

FM images of *pex3 atg1* cells producing Pex14-mCherry and 19 different peroxins N-terminally tagged with mGFP. The strains are grouped in functional groups. Cells were grown for 16 h on MM-O. Scale bar: 5 μm.

Pex15	membrane anchor for the AAA peroxins		✔		70,5
Pex1	AAA peroxin, recycling of peroxisomal signal receptors	✘			144
Pex6	AAA peroxin, recycling of peroxisomal signal receptors	✘			143
Pex19	receptor for newly synthetized PMPs	✘			65,5
Pex11	peroxisome proliferation	✘			54
Pex25	regulation of peroxisome size and number		✔		72
Pex27	regulation of peroxisome size and number	✘			71

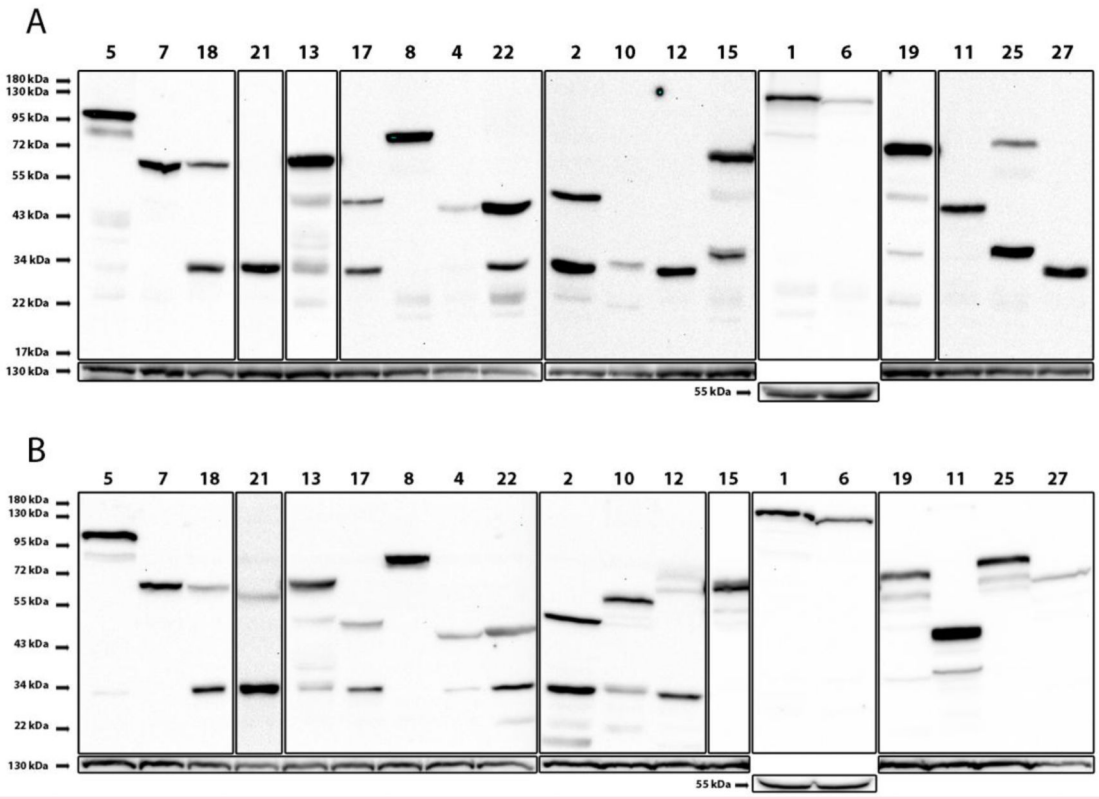

Figure 5. Western blot analysis of GFP-peroxin fusion proteins in *S. cerevisiae pex3 atg1* and WT cells.

(A) *pex3 atg1* and (B) WT controls producing N-terminal GFP fusion proteins under control of the *NOP1* promoter. Cells were grown for 16 h on MM-O. Western blots were decorated with anti-GFP antibodies. Different exposure times were used to optimally visualize the bands. Pyc1 (130 kDa) or G6PD (55 kDa) were used as loading controls.

Europe PMC Funders Author Manuscripts

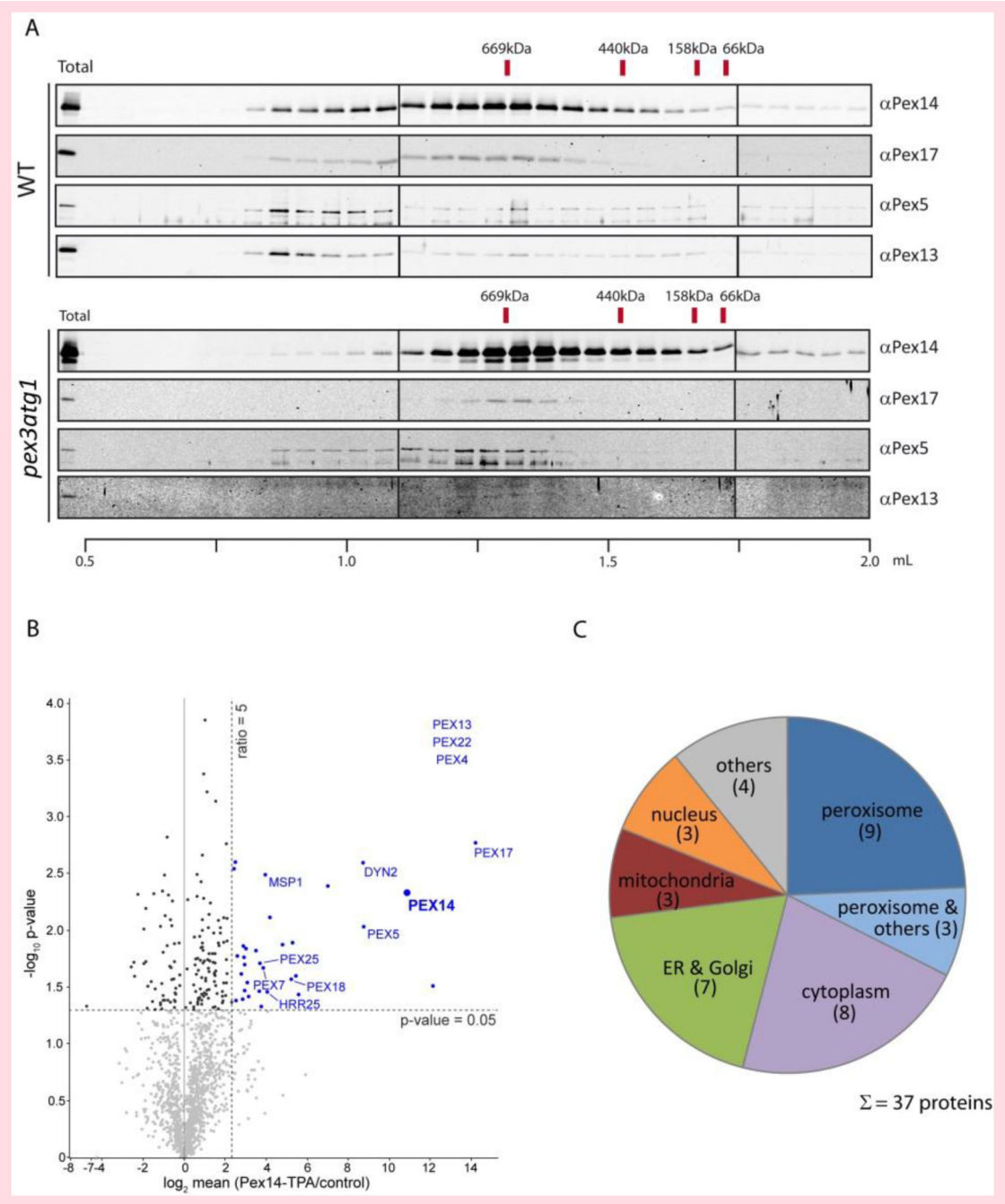

Figure 6. Pex14 is associated with other peroxisomal proteins in *pex3 atg1* cells.

(**A**) Pex14 protein complexes were isolated from solubilized total cell membranes prepared from WT and *pex3 atg1* cells and subjected to size-exclusion chromatography. In WT (top), two complexes are detected: a complex of about 700 kDa, which previously has been shown to exhibit the PTS1-pore activity, and a high-molecular weight complex, which also contained Pex13. In the absence of Pex3 (bottom), the 700 kDa complex is still formed while the higher molecular weight complex is absent. (**B**) Pex14 complexes were purified from *pex3 atg1* cells expressing either TPA-tagged or native, untagged Pex14 (control) and

analyzed by LC-MS. Mean $\log_2$ abundance ratios (Pex14-TPA/control; n = 3) were calculated and plotted against the p-value ($-\log_{10}$) determined for each protein (the full list of interactors is presented in Table S3). Proteins depicted in blue are specifically enriched in Pex14 complexes. Peroxisome-associated proteins found to be enriched are labelled. For Pex4, Pex13, and Pex22 (listed in the top right corner), mean ratios and p-values could not be calculated since they were only identified in complexes from Pex14-TPA-expressing cells. (**C**) Subcellular localization of proteins enriched in Pex14 complexes from *pex3 atg1* cells. Information is derived from Gene Ontology annotations for cellular compartment and entries in the *S. cerevisiae* Genome Database.

Europe PMC Funders Author Manuscripts

Europe PMC Funders Author Manuscripts

Table 1

Summary analysis of co-localization of various peroxins with Pex14

Peroxin	Function	Co-localization with Pex14			Calculated MW GFP fusion protein [kDa]
		No	Yes		
			Partial	Full	
Pex5	PTS1 receptor			✓	96,5
Pex7	PTS2 receptor		✓		69
Pex18	PTS2 co-receptor	✗			59
Pex21	PTS2 co-receptor	✗			60
Pex13	component of the docking complex		✓		70
Pex17	component of the docking complex		✓		50
Pex8	Matrix protein of importomer complex		✓		95
Pex4	ubiquitin conjugating enzyme (E2)		✓		48
Pex22	recruits Pex4 to peroxisome		✓		47
Pex2	peroxisomal ubiquitin ligase (E3)	✗			58
Pex10	peroxisomal ubiquitin ligase (E3)	✗			66
Pex12	peroxisomal ubiquitin ligase (E3)	✗			73
Pex15	membrane anchor for the AAA peroxins		✓		70,5
Pex1	AAA peroxin, recycling of peroxisomal signal receptors	✗			144
Pex6	AAA peroxin, recycling of peroxisomal signal receptors	✗			143
Pex19	receptor for newly synthetized PMPs	✗			65,5
Pex11	peroxisome proliferation	✗			54
Pex25	regulation of peroxisome size and number		✓		72
Pex27	regulation of peroxisome size and number	✗			71